Letter

Mirror symmetry at far edges of stability: The cases of ^{8}C and ^{8}He

S. Koyama,[1,2,3,4] D. Suzuki,[4] M. Assié,[5] L. Lalanne,[5,2] O. Sorlin,[2] T. Abe,[4,3] D. Beaumel,[5] Y. Blumenfeld,[5] L. Caceres,[2] F. De Oliveira Santos,[2] F. Delaunay,[6] F. Flavigny,[5,6] S. Franchoo,[5] J. Gibelin,[6] V. Girard-Alcindor,[2,5] J. Guillot,[5] F. Hammache,[5] O. Kamalou,[2] A. Kamenyero,[2] N. Kitamura,[3] V. Lapoux,[7] A. Lemasson,[2] A. Matta,[6] B. Mauss,[2] P. Morfouace,[2,8] M. Niikura,[1,4] H. Otsu,[4] J. Pancin,[2] T. Roger,[2] T. Y. Saito,[1,4] H. Sakurai,[1,4] C. Stodel,[2] and J-C. Thomas[2]

[1]*Department of Physics, The University of Tokyo, Hongo, Bunkyo-ku, Tokyo 113-0033, Japan*

[2]*Grand Accélérateur National d'Ions Lourds (GANIL), CEA/DRF-CNRS/IN2P3, Bd. Henri Becquerel, 14076 Caen, France*

[3]*Center for Nuclear Study, The University of Tokyo, Hongo, Bunkyo-ku, Tokyo 113-0033, Japan*

[4]*RIKEN Nishina Center, 2-1, Hirosawa, Wako, Saitama 351-0198, Japan*

[5]*Université Paris-Saclay, CNRS/IN2P3, IJCLab, 91405 Orsay, France*

[6]*Normandie Université, ENSICAEN, UNICAEN, CNRS/IN2P3, LPC Caen, 14000 Caen, France*

[7]*CEA, Centre de Saclay, IRFU, Service de Physique Nucléaire, 91191 Gif-sur-Yvette, France*

[8]*CEA, DAM, DIF, F-91297 Arpajon, France*

(Received 5 September 2022; revised 23 August 2023; accepted 22 December 2023; published 6 March 2024)

Missing mass spectroscopy of the unbound ^{8}C nucleus was performed by the one-neutron transfer ^{9}C(p, d) ^{8}C reaction at 55 MeV/nucleon. Besides the known ground state, two new resonant states were observed, the first at an excitation energy of 3.40(25) MeV with a width of 3.0(5) MeV, the second at 18.6(5) MeV with a width of 3.9(11) MeV. Spin and parity $J^{\pi} = 2^{+}$ were assigned to the first resonance from the distorted-wave Born approximation analysis of the experimental differential cross section. The excitation energy of the 2^{+} resonance in ^{8}C supports the persistence of the subshell closure at the semimagic number $Z = 6$, as is the case for $N = 6$. The mirror energy difference relative to the 2^{+} state in ^{8}He, $\Delta E_{x} = -0.14(25)$ MeV, is compatible with zero. Both states represent resonances in the continuum, unbound by about 1.4 and 6.9 MeV, respectively, above the particle thresholds. A simple theoretical model emphasizes the difference in unboundedness to account for a symmetry in mirror energies. This unique system is expected to provide a salient test of theoretical models, which include the treatment of the continuum.

DOI: 10.1103/PhysRevC.109.L031301

Symmetry is a fundamental concept in physics. In nuclear systems, protons and neutrons act almost equally under the nuclear force. This symmetry between proton and neutron, called charge symmetry, leads to the concept of isospin [1–3], which defines a proton and a neutron as different substates ($T_z = \pm 1/2$) of the same isospin $T = 1/2$ in the SU(2) group.

It is a fundamental question as to whether the isospin symmetry of the nuclear force is preserved in a many-body system as the atomic nucleus. The comparison between the level schemes of mirror nuclei, obtained by interchanging their proton and neutron numbers, offers the possibility to probe the so-called mirror symmetry [4–11]. In general their spectra show marked similarity, which is a proof that the isospin symmetry holds well in many-body isospin states. There exists, however, remarkable exceptions as in the alignment of pairs in rotational spectra, in the case of shape coexistence, or at the nuclear drip lines [8,9,11,12].

The evolution of mirror symmetry should, indeed, be scrutinized with care near the nuclear driplines. Weakly bound or unbound states built on low-ℓ orbitals are strongly coupled to scattering states, which in particular modifies the radial part of their wave functions. The increase of radial expansion gives rise to the spectacular phenomenon of halo structures [13,14], while the significant change between energies of mirror pairs, when one of the states is weakly bound or unbound, is known as the Thomas-Ehrman shift [15,16] effect. Theoretical studies suggest asymmetry in radii [17] or in configuration mixing [18–20] for mirror nuclei in the vicinity of the driplines.

In this Letter, we report on the discovery of a 2^{+} resonance in the proton-rich and unbound ^{8}C nucleus, with $Z = 6$ and $N = 2$. This allows us for the first time to study the mirror symmetry between two nuclei, ^{8}He and ^{8}C, via the 2^{+} states that are expected to be both strongly unbound. Indeed, the ground state of ^{8}He is bound by only 2.13 MeV, while the first 2^{+}_{1} state at 3.54(6) MeV [21] is already unbound by about 1.4 MeV with respect to the two-neutron emission threshold. It has a broad width (Γ) of 0.89(11) MeV [21]. The ^{8}C ground state is unbound by 3.48 MeV for $4p$ emission, forming a narrow resonance with $\Gamma = 130(50)$ keV [22,23]. Its 2^{+}_{1} state is expected to be unbound by about 7 MeV. In the two mirror nuclei, the 2^{+}_{1} state was proposed to originate from the simple $1p1h$ excitation from the $1p_{3/2}$ to the $1p_{1/2}$ orbital across the shell gap at the semimagicity of $N, Z = 6$ [24]. The mirror energy difference will be discussed and interpreted through a simple two-body model, that emphasizes the degree of unboundedness in preserving or breaking a symmetry in mirror energies.

The ^{8}C nucleus was studied by means of the neutron-transfer ^{9}C(p, d) ^{8}C reaction. We have used the missing mass method, where the excitation energy of the resonances as well

as their spin values are derived from information of the recoiling deuteron only. This method is far superior in efficiency to the invariant mass method, which would require here the detection of all four protons and the residual α particle. With a highly negative Q value of -12 MeV, this (p, d) reaction, carried out at 55 MeV/nucleon, gives deuteron energies higher than 16 MeV. Therefore, a rather thick target can be used. Our choice was oriented to a cryogenic hydrogen target of the order of 1 mm, which enables higher statistics and lower backgrounds than using a CH_2 target with a thickness that gives an equivalent energy resolution [5,11,25–27].

The experiment was carried out at the LISE beam line of GANIL. A primary beam of ^{12}C was fragmented by a 2.2-mm thick Be target at 75 MeV/nucleon to produce ^{9}C at about 55 MeV/nucleon and its isotones of $N = 3$. These nuclei were selected by the LISE fragment separator [28] equipped with a wedge-shaped Be degrader of 1.0 mm in thickness. To reduce the ratio of the isotones, the Wien filter was operated at an electric field of 250 V/m. The cocktail beam was delivered to the final focal plane of LISE and impinged on a 1.5-mm thick (10.5 mg/cm^2) cryogenic liquid hydrogen target [29], in which the (p, d) reactions occurred. To monitor the incident position and angle of the beam particles on target, a pair of multiwire proportional chambers CATS [30] with a typical position resolution of 1 mm r.m.s. was placed upstream of the target at a distance of 68 and 119 cm, respectively. The time difference of the CATS signal with respect to the radio frequency signal of the cyclotrons was used to identify the mass number of beam particles. The purity of ^{9}C was around 5% for a total intensity of 1.3×10^5 pps. The isotones include ^{8}B (10%), ^{7}Be (65%), and ^{6}Li (20%). An array of six telescopes of the charged-particle MUST2 detector was used to detect recoiling deuterons from 2° to 36°, as described in Fig. 1 of Ref. [27]. Each telescope consisted of a double-sided silicon strip detector (DSSD) followed by CsI(Tl) detectors. The DSSD has an active area of 98×98 mm^2 with a thickness of 300 μm. Each surface of the detector is segmented into 128 strips with a 0.76 mm pitch. The energy resolution was about 40 keV FWHM for 5.5-MeV α particles of an ^{241}Am standard source. Behind the DSSD, 16 CsI(Tl) crystals, mounted in a 4×4 matrix, cover an area of 122×122 mm^2. The total kinetic energy was deduced from the sum of the energies measured by the DSSD and the CsI(Tl) detectors. The particle identification was performed by the E-ΔE method. The scattering angle of a recoiling particle was obtained from the hit position measured by the DSSDs, after correcting for the position and angle of the incident ion on target.

The excitation energy (E_x) of ^{8}C and the center-of-mass scattering angle ($\theta_{c.m.}$) were reconstructed by means of the missing mass method, using the energy and angle of the recoiling deuteron. The excitation energy spectrum, integrated up to $\theta_{c.m.} = 45°$, thus obtained is shown in Fig. 1. Here the background from the target cell was subtracted by using the data taken without liquid hydrogen. Besides the ground-state resonance centered at 0 MeV, a tailing structure over a few MeV (centered near 3 MeV) and a broad peak at higher energies (near 18 MeV) are visible in the spectrum, indicating two new resonances. Owing to our present energy resolution and the large decay width of the excited resonance, the ground and first excited states are not clearly separated. Note that the tailing structure is not due to a possible asymmetric shape of the ground-state resonance. First, our experimental response function is symmetric with a resolution of 0.50(5) MeV r.m.s. This is validated by the NPTOOL simulation [31] and also by the reference ^{12}C$(p, d)^{11}$C reaction, measured in the same experimental conditions [29], and in which a single symmetric isolated peak can be observed. This resolution is mainly governed by the energy resolution of the CsI(Tl) detectors and by the uncertainty of the energy loss of the recoiling particles before exiting from the target. Second, the ground-state resonance has a decay width of 0.13(5) MeV and a symmetric shape in Refs. [22,23]. After subtracting the symmetric fitting function for the ground state, as described later, the spectrum in Fig. 1(b) clearly shows an asymmetric broad resonance centered around 3 MeV, on top of nonresonant breakup components.

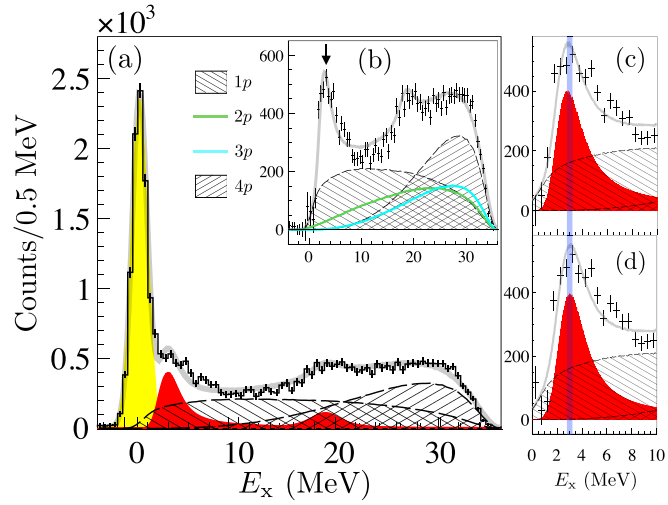

FIG. 1. Excitation energy spectra of ^{8}C. (a) Angle-integrated spectrum up to $\theta_{c.m.} = 45°$. The fit curve (depicted by the corresponding gray error band) is shown together with the response functions for the ground state (in yellow), the excited states (in red), and for nonresonant backgrounds (hatched areas). (b) The same spectrum after subtracting the response function for the ground state. The new 2^+ resonance is indicated by the arrow. To visualize the spectral shapes, the nonresonant backgrounds are plotted with arbitrary scaling factors. (c), (d) Ground-state subtracted spectra by assuming the experimental resolution of 0.45 MeV and 0.55 MeV, respectively. The peak position of the original fit curve is indicated by the blue bands for comparison. The band width corresponds to the error of E_x (±0.25 MeV).

The spectrum has been fitted by means of three resonances and nonresonant breakup components corresponding to $1p$ to $4p$ emissions. Resonance centroids and widths of the ground and 18-MeV states were fitted by standard Voigt functions that are convolutions of a Breit-Wigner and a Gaussian distribution. Owing to the broad width of the 3-MeV state, as compared to its excitation energy value, the Voigt function was modified to consider an energy-dependent decay width Γ, which induces an asymmetric shape. Based on the R-matrix formalism [32], we adopted $\Gamma(E_x) = 2P_l(E_x)\gamma^2$, with the penetrability P_l at a given E_x for the orbital angular momentum

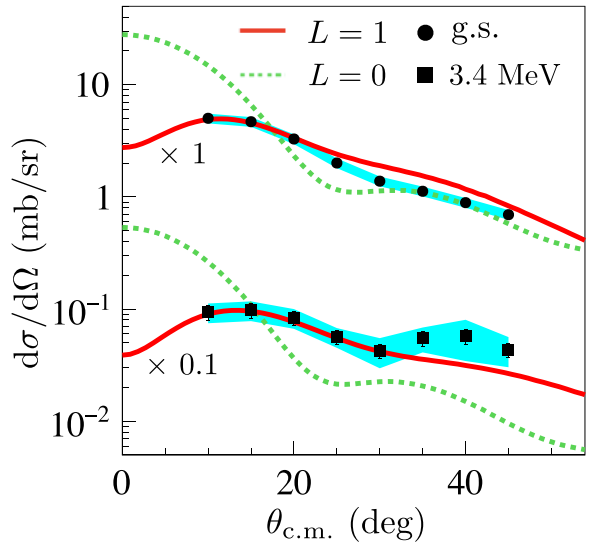

FIG. 2. Differential cross sections of the ground (circle) and first excited states (square, scaled by 0.1) of ^{8}C derived from the ^{9}C(p, d)^{8}C reaction at 55 MeV/nucleon. The data are compared to the DWBA calculations for the $L = 1$ (solid line) and $L = 0$ (dotted line) neutron removal from the $1p_{3/2}$ and $1s_{1/2}$ orbitals. Note that the DWBA calculations for $1p_{3/2}$ and $1p_{1/2}$ orbitals are almost the same up to 50°. Therefore, only that for $1p_{3/2}$ is shown. The statistical (systematic) uncertainties are indicated by the error bars (shaded area).

l and with the reduced width γ. The decay channel was assumed to be ^{7}B $+p$, with $l = 1$ corresponding to the $1p$ emission from the p shell. The shapes of the nonresonant breakup components from $1p$–$4p$ were calculated for uniform phase space [11,25]. Here the geometrical acceptance and the energy resolutions of the detectors were taken into account. The fit with all $1p$–$4p$ leads to zero amplitudes for $2p$ and $3p$. The combination of the $1p$ and $4p$ components alone can reproduce the background for a whole energy range of the spectrum. We checked other combinations of the $1p$–$4p$ components by restricting the fit to a specific combination, for instance, $2p + 4p$. The reduced χ^2 value of $\chi^2/\mathrm{ndf} = 111/71 = 1.56$ for the adopted fit is found to be the smallest.

The obtained reduce χ^2 value is larger than the unity, which can be due to the imperfection of the response function. To deal with this issue, we adopted the same method as in Ref. [33]. The E_x spectrum was fitted by scaling the error of each data point by $\sqrt{1.56} = 1.25$ to obtain $\chi^2/\mathrm{ndf} = 1$. As a result of this fit, resonance energies and widths are $E_x = 3.40(25)$ MeV and $\Gamma = 3.0(5)$ MeV for the first excited resonance, and $E_x = 18.6(5)$ MeV and $\Gamma = 3.9(11)$ MeV for the second. Note that the upper limit of Γ is constrained by the higher-energy tail, as seen in Figs. 1(c) and 1(d). The fitting errors in the parentheses are defined by one standard deviation. For confirmation, we checked the variation of the E_x value by repeating the fits with one of the other parameters fixed to the minimum or to the maximum within their errors. The parameters include Γ of the first excited state and of the ground state, the amplitudes of the $1p$ and $4p$ components and the E_x resolution. In all cases, the resulting E_x values are found within the adopted error of ± 0.25 MeV.

Experimental differential cross sections, shown for the ground state and the resonance at 3.4 MeV in Fig. 2, have been obtained by fitting the excitation energy spectrum at each angle in the same way as the angle-integrated spectrum mentioned above. Note that E_x obtained for the angle-gated spectra ranges from 3.29–3.55 MeV and agree with the adopted value. The shaded area denotes the systematic uncertainties arising from the magnitude of the nonresonant components. The diffractive pattern of the 3.4-MeV state is similar to that of the ground 0^+ ($0^+_{g.s.}$) state, indicating the same transferred angular momentum from the initial $3/2^-$ state of ^{9}C. Distorted-wave Born approximation (DWBA) calculations were performed using the DWUCK5 code [34] and the global nucleon potential CH89 [35] for both entrance and exit channels. While the final state is a broad resonance, CH89 was used in similar situations in previous studies [36,37]. The adiabatic approximation [38] was applied to the exit channel to treat the deuteron breakup. The experimental angular distributions from the (p, d) reaction are well reproduced using an $L = 1$ transferred angular momentum from the $1p_{3/2}$ orbital, while the calculation using $L = 0$ ($1s_{1/2}$) is inconsistent. The spectroscopic factor (C^2S) is deduced to be 0.69(14) for the ground state and 0.15(3) for the 3.4-MeV state. The spin and parity of the latter are constrained to 0^+, 1^+, or 2^+ from $L = 1$. Shell model calculations were carried out by the KSHELL [39] code using the CK [40] and YSOX [41] interactions, both providing C^2S of about 0.87 for the 0^+_{gs} state. With both interactions, only the 2^+_1 state has a consistent C^2S (0.13 with CK and 0.10 with YSOX) with the experimental result. The C^2S of other states are too small for observation. We thus assign 2^+ to the new state at 3.4 MeV.

To examine the magicity of ^{8}C and its symmetry to ^{8}He, their $E_x(2^+_1)$ energy and energy difference $\Delta E_x = E_x(^{8}\mathrm{C}) - E_x(^{8}\mathrm{He})$, are compared in Figs. 3(c) and 3(d), respectively, to values of even-even mirror nuclei. Data are sorted with isospin values from $T = 1$–3 in order to emphasize the role of the isospin asymmetry. As for ^{8}He, we adopt $E_x(2^+_1) = 3.54(6)$ MeV from Ref. [21]. In this plot, the doubly or singly magic nuclei are characterized by the high $E_x(2^+_1)$ values in the respective isospin series. Together with ^{36}Ca at $Z = 20$ [11], the $E_x(2^+_1)$ of ^{8}C lies at high energy in the $T = 2$ series. This supports that the subshell closure holds at the proton semimagic number $Z = 6$, as suggested for ^{8}C by a theoretical study [24]. Note that unbound states are in general prone to energy shifts, and the excitation energy alone may not be enough to conclude. As for the $N = 6$ closure in ^{8}He, a C^2S value of 2.9(9) has been derived in Refs. [46,47] for the $1p_{3/2}$ orbital, using the ^{8}He(p, d)^{7}He reaction. This value is consistent, within the error bar, with its full occupancy of 4, after having taken the nominal quenching factor of about 2/3.

As shown in Fig. 3(d), the mirror energy difference $\Delta E_x = E_x(^{8}\mathrm{C}) - E_x(^{8}\mathrm{He}) = -0.14(25)$ MeV fits into the nominal range of other nuclei. This preserved symmetry comes *a priori* as a surprise, since the 2^+_1 state in ^{8}C can be strongly influenced by the energy shift, as having by far the broadest width observed among all $T = 1$–3 nuclei. Even if challenging in a many-body system, the theoretical implementation of resonances in the continuum is requested to understand

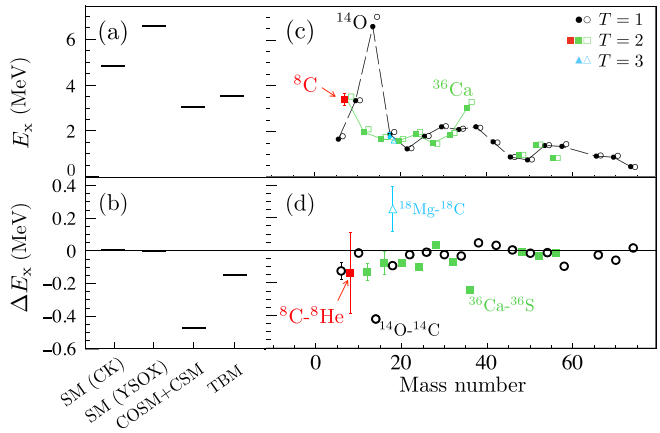

FIG. 3. (a) $E_x(2_1^+)$ of ^{8}C and (b) ΔE_x with respect to ^{8}He obtained from the shell model (SM) calculations using the CK [40] and YSOX [41] interactions, the cluster orbital shell model with the complex scaling method (COSM + CSM) [24] and the two-body model (TBM) [42]. (c) Experimental $E_x(2_1^+)$ and (d) ΔE_x of even-even mirror nuclei from Refs. [10,43–45]. The data of proton-rich (filled symbols) and neutron-rich (open symbols) nuclei are sorted by $T = 1$ (circle), 2 (square), and 3 (triangles), while doubly or singly magic nuclei are indicated.

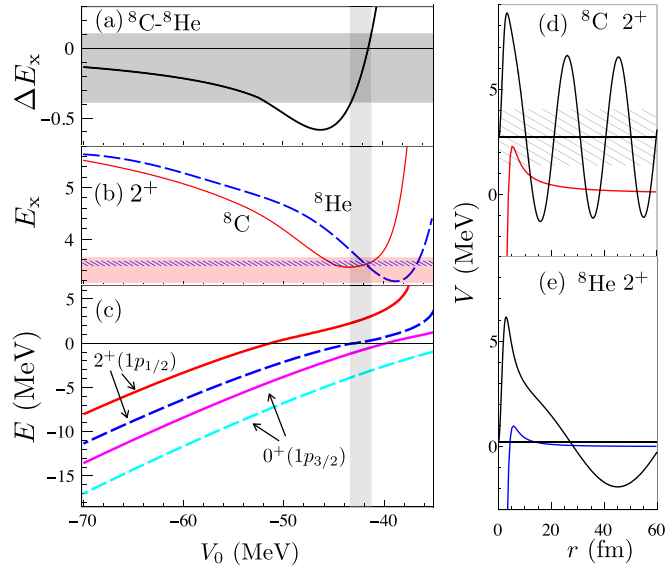

FIG. 4. Results of the two-body model calculation. (a) Mirror energy difference $\Delta E_x(2_1^+)$ and (b) $E_x(2_1^+)$ are plotted for the potential depth V_0. The optimal V_0 (vertical band) to reproduce the experimental data (shaded horizontal band for ^{8}C, hatched horizontal band for ^{8}He) is indicated. The band widths for the latter denote the experimental errors. (c) Eigen energies of the $1p_{3/2}$ (0^+) and $1p_{1/2}$ (2^+) orbitals of ^{8}C (solid lines) and ^{8}He (dashed lines). (d) Radial wavefunction of the 2^+ state in ^{8}C for the optimal $V_0 = 42$ MeV is shown in an arbitrary unit (black curve). The eigen energy (horizontal line) and width (shaded band) are visualized with the potential (red curve). (e) Same plot for ^{8}He, with the potential shown by the blue curve.

the situation. Shell model calculations using bound-state wave functions [40,41] suggest the 2_1^+ state to be a $1p1h$ excitation from the $1p_{3/2}$ to $1p_{1/2}$ orbital and be located at $E_x(2_1^+)$ higher by a few MeV as compared to experiment [Fig. 3(a)]. The COSM + CSM calculation [24], which can treat many-body resonances, also supports the $1p1h$ configuration, but places the $E_x(2_1^+)$ of ^{8}C at a lower excitation energy, in agreement with the experimental value.

To clarify the importance of the states being unbound in ^{8}C and ^{8}He, we introduce the two-body model (TBM) [42], in which the 2_1^+ states are represented by a $1p1h$ configuration with a valence proton or neutron and a hole into the $Z, N = 6$ subshell closed core. This model may be a good approximation as all theoretical models discussed here predict a dominating $1p1h$ structure. By this simplification, two-body resonances can be handled fully and exact numerical solutions for both bound and unbound states can be obtained. In tradeoff, the many-body effects such as the pairing correlations are treated in the simplest way with a one-body mean-field potential. The microscopic treatment of all decay channels, extremely difficult in general, is out of scope in this model. The time-independent one-dimensional Schrödinger equation is solved by the Numerov method where the inner and outer wave functions are matched at a given distance of 10 fm. The outer wave functions of bound (unbound) states are asymptotically vanishing to zero (the Coulomb wave functions). As for resonant states, the phase shift is calculated with a given potential. The resonance energies are defined by the phase shift (δ) crossing 90°. The corresponding width is defined by $2/(d\delta/dE)$ ($\delta = 90°$).

The one-body potential consists of the Woods-Saxon, including centrifugal (V_L), spin-orbit and Coulomb (V_C) potentials. The $1p_{3/2}$ and $1p_{1/2}$ states of Fig. 4(c) are representative of the $0^+_{\text{g.s.}}$ and 2_1^+ states, respectively. The parametrization of Ref. [3] was used for the radius ($r = 2.54$ fm), diffuseness ($a = 0.67$ fm) and spin-orbit potential ($V_{\text{SO}} = 7.5$ MeV). The depth of the WS potential V_0 was varied to trail the behavior from deeply bound states to resonances. The evolution of $E_x(2_1^+)$ is displayed in Fig. 4(b) as a function of V_0, which varies from -70 (deep) to -35 MeV (shallow). At around -70 MeV, the $0^+_{\text{g.s.}}$ and 2_1^+ states are deeply bound. $E_x(2_1^+)$ is much higher than experimentally, as for shell model calculations given in Fig. 3(a). A ΔE_x value of about -0.1 MeV is found, indicating a good symmetry in mirror energies, as for the vast majority of data shown in Fig. 3(d).

As the potential gets shallower, $E_x(2_1^+)$ of both ^{8}C and ^{8}He progressively reduces, while ΔE_x is increasing smoothly. This trend, continues until reaching about -52 MeV, where the $1p_{1/2}$ orbital in ^{8}C [red color in Fig. 4(c)] becomes unbound first. This induces a steeper decrease of its $E_x(2_1^+)$, herewith increasing the difference of energy ($|\Delta E_x|$) between the two nuclei. This energy gain near the threshold occurs as the proton starts tunneling through the potential ($V_L + V_C$) barriers. This effect, vastly studied for s-wave nucleons [42,48], turns out to be also important in the case of a p wave. At this point, the symmetry in mirror energies is thus significantly broken with $|\Delta E_x| \simeq 0.6$ MeV.

An abrupt change occurs around -43 MeV. Here, the $1p_{1/2}$ orbital of ^{8}He also becomes unbound, reducing in turn its $E_x(2_1^+)$, while that of ^{8}C goes far beyond the barrier

top, increasing $E_x(2_1^+)$. Near -42 MeV, the $|\Delta E_x|$ value reaches the experimental one [gray area of Fig. 4(a)] and the symmetry in mirror energies is restored. Note that the qualitative behavior of ΔE_x as a function of V_0 is the same in case the parameters of r, a, and V_{SO} are changed by $\pm 10\%$.

At the optimal V_0 value, the radial wave functions of the 2_1^+ $(1p_{1/2})$ states are shown in Figs. 4(d) and 4(e) in an arbitrary unit, respectively. The wave functions significantly differ between ^{8}C and ^{8}He, especially at asymptotic distance, reflecting the potential shapes and the energies relative to the barrier top. The ^{8}C 2_1^+ state emerges as a broad resonance above the Coulomb and centrifugal barriers, while the ^{8}He 2_1^+ state lies as a narrow resonance below the centrifugal barrier. This difference relative to the barrier top leads to the restoration of the mirror energies, which is in contrast to the deep binding cases, where the similarity in wave functions accounts for the symmetry in mirror energies.

In summary, the unbound ^{8}C nucleus was studied at GANIL via the ^{9}C(p, d) reaction at 55 MeV/nucleon. The excitation energy spectrum was obtained by the missing mass method using the MUST2 telescopes. Two resonances were discovered, one at 3.40(25) MeV with a width of 3.0(5) MeV and the other at 18.6(5) MeV with 3.9(11) MeV. The spin and parity of the former were determined to be 2^+, based on the shape and amplitude of the differential cross section. E_x of the newly found 2^+ state is higher compared to the known $E_x(2_1^+)$ of proton-rich even-even nuclei with $T = 2$, supporting that the subshell closure $Z = 6$ holds in ^{8}C. The 2_1^+ states of ^{8}C and ^{8}He lie at similar energies, leading to a small energy difference $\Delta E_x = -0.14(25)$ MeV. This points to a good symmetry in mirror energies, despite the width of the 2_1^+ state in ^{8}C [$\Gamma = 3.0(5)$ MeV] is the broadest among the known 2_1^+ states of even-even nuclei, except for ^{4}He. The 2^+ states in the mirror nuclei were calculated by the two-body model to treat resonances. It was shown that the 2^+ state in ^{8}C is a broad resonance above the Coulomb and centrifugal barriers, while the ^{8}He resonance lies just below the centrifugal barrier top. As compared to calculations for bound states, both 2^+ energies are lowered in concert by about a few MeV. The symmetry in mirror energies is preserved owing to the nature of the barriers in ^{8}C ($V_L + V_C$) and ^{8}He (V_L only), and relative binding energy to their top (above or just below). These nuclei offer a unique case of close-to-doubly-magic nuclei, both involving resonances in the continuum. A more explicit treatment of the many-body correlations with the continuum is required. A good understanding of such examples is essential to model other nuclei close or beyond the drip line.

The authors thank the accelerator staff and the technical staff of GANIL. Discussions with N. Itagaki, M. Ito, Y. Kanada-En'yo, N. Hinohara, T. Myo, H. Sagawa, Y. Sakurada, and Y. Tanimura are gratefully acknowledged. S.K. was supported by the JSPS Grant-in-Aid for JSPS Research Fellows JP16J04726. This work was supported by the JSPS KAKENHI Grants No. JP19H01914 and No. JP21K03564

[1] W. Heisenberg, Z. Phys. **77**, 1 (1932).
[2] E. Wigner, Phys. Rev. **51**, 106 (1937).
[3] A. Bohr and B. Mottelson, *Nuclear Structure* (Benjamin, Boston, 1969), Vol. I.
[4] T. Teranishi, S. Kubono, H. Yamaguchi, J. He, A. Saito, H. Fujikawa, G. Amadio, M. Niikura, S. Shimoura, Y. Wakabayashi, S. Nishimura, M. Nishimura, J. Moon, C. Lee, A. Odahara, D. Sohler, L. Khiem, Z. Li, G. Lian, and W. Liu, Phys. Lett. B **650**, 129 (2007).
[5] D. Suzuki, H. Iwasaki, D. Beaumel, L. Nalpas, E. Pollacco, M. Assié, H. Baba, Y. Blumenfeld, N. De Séréville, A. Drouart, S. Franchoo, A. Gillibert, J. Guillot, F. Hammache, N. Keeley, V. Lapoux, F. Maréchal, S. Michimasa, X. Mougeot, I. Mukha, H. Okamura, H. Otsu, A. Ramus, P. Roussel-Chomaz, H. Sakurai, J.-A. Scarpaci, O. Sorlin, I. Stefan, and M. Takechi, Phys. Rev. Lett. **103**, 152503 (2009).
[6] I. Stefan, F. de Oliveira Santos, O. Sorlin, T. Davinson, M. Lewitowicz, G. Dumitru, J. C. Angélique, M. Angélique, E. Berthoumieux, C. Borcea, R. Borcea, A. Buta, J. M. Daugas, F. de Grancey, M. Fadil, S. Grévy, J. Kiener, A. Lefebvre-Schuhl, M. Lenhardt, J. Mrazek, F. Negoita, D. Pantelica, M. G. Pellegriti, L. Perrot, M. Ploszajczak, O. Roig, M. G. Saint Laurent, I. Ray, M. Stanoiu, C. Stodel, V. Tatischeff, and J. C. Thomas, Phys. Rev. C **90**, 014307 (2014).
[7] T. B. Webb, S. M. Wang, K. W. Brown, R. J. Charity, J. M. Elson, J. Barney, G. Cerizza, Z. Chajecki, J. Estee, D. E. M. Hoff, S. A. Kuvin, W. G. Lynch, J. Manfredi, D. McNeel, P. Morfouace, W. Nazarewicz, C. D. Pruitt, C. Santamaria, J. Smith, L. G. Sobotka, S. Sweany, C. Y. Tsang, M. B. Tsang, A. H. Wuosmaa, Y. Zhang, and K. Zhu, Phys. Rev. Lett. **122**, 122501 (2019).
[8] V. Girard-Alcindor, I. Stefan, F. de Oliveira Santos, O. Sorlin, D. Ackermann, P. Adsley, J. C. Angélique, M. Assié, M. Assunção, D. Beaumel, E. Berthoumieux, R. Borcea, L. Cáceres, I. Celikovic, M. Ciemala, V. Chudoba, G. D'Agata, F. de Grancey, G. Dumitru, F. Flavigny, C. Fougères, S. Franchoo, A. Georgiadou, N. Goyal, S. Grévy, J. Guillot, V. Guimaraes, F. Hammache, O. Kamalou, J. Kiener, S. Koyama, L. Lalanne, V. Lapoux, I. Matea, A. Matta, A. Meyer, N. Michel, P. Morfouace, J. Mrazek, F. Negoita, M. Niikura, D. Pantelica, L. Perrot, C. Petrone, J. Piot, C. Portail, T. Roger, F. Rotaru, A. M. Sánchez Benítez, N. de Séréville, M. Stanoiu, C. Stodel, K. Subotic, D. Suzuki, V. Tatischeff, J. C. Thomas, P. Ujic, and D. Verney, Eur. Phys. J. A **57**, 93 (2021).
[9] V. Girard-Alcindor, A. Mercenne, I. Stefan, F. de Oliveira Santos, N. Michel, M. Płoszajczak, M. Assié, A. Lemasson, E. Clément, F. Flavigny *et al.*, Phys. Rev. C **105**, L051301 (2022).
[10] Y. Jin, C. Y. Niu, K. W. Brown, Z. H. Li, H. Hua, A. K. Anthony, J. Barney, R. J. Charity, J. Crosby, D. Dell'Aquila, J. M. Elson, J. Estee, M. Ghazali, G. Jhang, J. G. Li, W. G. Lynch, N. Michel, L. G. Sobotka, S. Sweany, F. C. E. Teh, A. Thomas, C. Y. Tsang, M. B. Tsang, S. M. Wang, H. Y. Wu, C. X. Yuan, and K. Zhu, Phys. Rev. Lett. **127**, 262502 (2021).
[11] L. Lalanne, O. Sorlin, A. Poves, M. Assié, F. Hammache, S. Koyama, D. Suzuki, F. Flavigny, V. Girard-Alcindor, A. Lemasson, A. Matta, T. Roger, D. Beaumel, Y. Blumenfeld, B. A. Brown, F. D. O. Santos, F. Delaunay, N. de Séréville, S. Franchoo, J. Gibelin, J. Guillot, O. Kamalou, N. Kitamura,

V. Lapoux, B. Mauss, P. Morfouace, M. Niikura, J. Pancin, T. Y. Saito, C. Stodel, and J.-C. Thomas, Phys. Rev. Lett. **129**, 122501 (2022).
[12] D. D. Warner, M. A. Bentley, and P. V. Isacker, Nat. Phys. **2**, 311 (2006).
[13] I. Tanihata, H. Hamagaki, O. Hashimoto, Y. Shida, N. Yoshikawa, K. Sugimoto, O. Yamakawa, T. Kobayashi, and N. Takahashi, Phys. Rev. Lett. **55**, 2676 (1985).
[14] P. G. Hansen and B. Jonson, Europhys. Lett. **4**, 409 (1987).
[15] J. B. Ehrman, Phys. Rev. **81**, 412 (1951).
[16] R. G. Thomas, Phys. Rev. **88**, 1109 (1952).
[17] T. Myo and K. Katō, Prog. Theor. Exp. Phys. **2014**, 83D01 (2014).
[18] L. V. Grigorenko, I. G. Mukha, I. J. Thompson, and M. V. Zhukov, Phys. Rev. Lett. **88**, 042502 (2002).
[19] L. V. Grigorenko, T. A. Golubkova, and M. V. Zhukov, Phys. Rev. C **91**, 024325 (2015).
[20] N. Michel, W. Nazarewicz, and M. Płoszajczak, Phys. Rev. C **82**, 044315 (2010).
[21] M. Holl, R. Kanungo, Z. Sun, G. Hagen, J. Lay, A. Moro, P. Navrátil, T. Papenbrock, M. Alcorta, D. Connolly, B. Davids, A. Diaz Varela, M. Gennari, G. Hackman, J. Henderson, S. Ishimoto, A. Kilic, R. Krücken, A. Lennarz, J. Liang, J. Measures, W. Mittig, O. Paetkau, A. Psaltis, S. Quaglioni, J. Randhawa, J. Smallcombe, I. Thompson, M. Vorabbi, and M. Williams, Phys. Lett. B **822**, 136710 (2021).
[22] R. J. Charity, J. M. Elson, J. Manfredi, R. Shane, L. G. Sobotka, Z. Chajecki, D. Coupland, H. Iwasaki, M. Kilburn, J. Lee, W. G. Lynch, A. Sanetullaev, M. B. Tsang, J. Winkelbauer, M. Youngs, S. T. Marley, D. V. Shetty, A. H. Wuosmaa, T. K. Ghosh, and M. E. Howard, Phys. Rev. C **82**, 041304(R) (2010).
[23] R. J. Charity, J. M. Elson, J. Manfredi, R. Shane, L. G. Sobotka, B. A. Brown, Z. Chajecki, D. Coupland, H. Iwasaki, M. Kilburn, J. Lee, W. G. Lynch, A. Sanetullaev, M. B. Tsang, J. Winkelbauer, M. Youngs, S. T. Marley, D. V. Shetty, A. H. Wuosmaa, T. K. Ghosh, and M. E. Howard, Phys. Rev. C **84**, 014320 (2011).
[24] T. Myo, M. Odsuren, and K. Kato, Phys. Rev. C **104**, 044306 (2021).
[25] D. Suzuki, Eur. Phys. J. A **48**, 130 (2012).
[26] D. Suzuki, H. Iwasaki, D. Beaumel, M. Assié, H. Baba, Y. Blumenfeld, F. de Oliveira Santos, N. de Séréville, A. Drouart, S. Franchoo, J. Gibelin, A. Gillibert, S. Giron, S. Grévy, J. Guillot, M. Hackstein, F. Hammache, N. Keeley, V. Lapoux, F. Maréchal, A. Matta, S. Michimasa, L. Nalpas, F. Naqvi, H. Okamura, H. Otsu, J. Pancin, D. Y. Pang, L. Perrot, C. M. Petrache, E. Pollacco, A. Ramus, W. Rother, P. Roussel-Chomaz, H. Sakurai, J.-A. Scarpaci, O. Sorlin, P. C. Srivastava, I. Stefan, C. Stodel, Y. Tanimura, and S. Terashima, Phys. Rev. C **93**, 024316 (2016).
[27] L. Lalanne, O. Sorlin, M. Assié, F. Hammache, N. de Séréville, S. Koyama, D. Suzuki, F. Flavigny, D. Beaumel, Y. Blumenfeld, B. A. Brown, F. D. O. Santos, F. Delaunay, S. Franchoo, J. Gibelin, V. Girard-Alcindor, J. Guillot, O. Kamalou, N. Kitamura, V. Lapoux, A. Lemasson, A. Matta, B. Mauss, P. Morfouace, M. Niikura, J. Pancin, A. Poves, T. Roger, T. Saito, C. Stodel, and J.-C. Thomas, Phys. Rev. C **103**, 055809 (2021).
[28] R. Anne and A. C. Mueller, Nucl. Instrum. Meth. Phys. Res. B **70**, 276 (1992).
[29] S. Koyama, D. Suzuki, M. Assié, N. Kitamura, L. Lalanne, M. Niikura, H. Otsu, T. Saito, and O. Sorlin, Nucl. Instrum. Meth. Phys. Res. A **1010**, 165477 (2021).
[30] S. Ottini-Hustache, C. Mazur, F. Auger, A. Musumarra, N. Alamanos, B. C. n, A. Gillibert, A. Lagoyannis, O. Maillard, E. Pollacco, J. Sida, and M. Riallot, Nucl. Instrum. Meth. Phys. Res. A **431**, 476 (1999).
[31] A. Matta, P. Morfouace, N. de Séréville, F. Flavigny, M. Labiche, and R. Shearman, J. Phys. G: Nucl. Part. Phys. **43**, 045113 (2016).
[32] P. Descouvemont and D. Baye, Rep. Prog. Phys. **73**, 036301 (2010).
[33] J. Zenihiro, H. Sakaguchi, T. Murakami, M. Yosoi, Y. Yasuda, S. Terashima, Y. Iwao, H. Takeda, M. Itoh, H. P. Yoshida, and M. Uchida, Phys. Rev. C **82**, 044611 (2010).
[34] NEA repository, https://www.oecdnea.org/tools/abstract/detail/nesc9872.
[35] R. Varner, W. Thompson, T. McAbee, E. Ludwig, and T. Clegg, Phys. Rep. **201**, 57 (1991).
[36] A. A. Korsheninnikov, M. S. Golovkov, A. Ozawa, E. A. Kuzmin, E. Y. Nikolskii, K. Yoshida, B. G. Novatskii, A. A. Ogloblin, I. Tanihata, Z. Fulop, K. Kusaka, K. Morimoto, H. Otsu, H. Petrascu, and F. Tokanai, Phys. Rev. Lett. **82**, 3581 (1999).
[37] F. Skaza, V. Lapoux, N. Keeley, N. Alamanos, E. C. Pollacco, F. Auger, A. Drouart, A. Gillibert, D. Beaumel, E. Becheva, Y. Blumenfeld, F. Delaunay, L. Giot, K. W. Kemper, L. Nalpas, A. Obertelli, A. Pakou, R. Raabe, P. Roussel-Chomaz, J.-L. Sida, J.-A. Scarpaci, S. Stepantsov, and R. Wolski, Phys. Rev. C **73**, 044301 (2006).
[38] J. D. Harvey and R. C. Johnson, Phys. Rev. C **3**, 636 (1971).
[39] N. Shimizu, T. Mizusaki, Y. Utsuno, and Y. Tsunoda, Comput. Phys. Commun. **244**, 372 (2019).
[40] S. Cohen and D. Kurath, Nucl. Phys. **73**, 1 (1965).
[41] C. Yuan, T. Suzuki, T. Otsuka, F. Xu, and N. Tsunoda, Phys. Rev. C **85**, 064324 (2012).
[42] C. R. Hoffman, B. P. Kay, and J. P. Schiffer, Phys. Rev. C **94**, 024330 (2016).
[43] National nuclear data center, https://www.nndc.bnl.gov/.
[44] R. Yajzey, M. Bentley, E. Simpson, T. Haylett, S. Uthayakumaar, D. Bazin, J. Belarge, P. Bender, P. Davies, B. Elman, A. Gade, H. Iwasaki, D. Kahl, N. Kobayashi, S. Lenzi, B. Longfellow, S. Lonsdale, E. Lunderberg, L. Morris, D. Napoli, X. Pereira-Lopez, F. Recchia, J. Tostevin, R. Wadsworth, and D. Weisshaar, Phys. Lett. B **823**, 136757 (2021).
[45] A. Fernández, A. Jungclaus, P. Doornenbal, M. Bentley, S. Lenzi, D. Rudolph, F. Browne, M. Cortés, T. Koiwai, R. Taniuchi, V. Vaquero, K. Wimmer, T. Arici, N. Imai, N. Kitamura, B. Longfellow, R. Lozeva, B. Mauss, D. Napoli, M. Niikura, X. Pereira-Lopez, S. Pigliapoco, A. Poves, F. Recchia, P. Ruotsalainen, H. Sakurai, S. Uthayakumaar, R. Wadsworth, and R. Yajzey, Phys. Lett. B **823**, 136784 (2021).
[46] N. Keeley, F. Skaza, V. Lapoux, N. Alamanos, F. Auger, D. Beaumel, E. Becheva, Y. Blumenfeld, F. Delaunay, A. Drouart, A. Gillibert, L. Giot, K. Kemper, L. Nalpas, A. Pakou, E. Pollacco, R. Raabe, P. Roussel-Chomaz, K. Rusek, J.-A. Scarpaci, J.-L. Sida, S. Stepantsov, and R. Wolski, Phys. Lett. B **646**, 222 (2007).
[47] V. Lapoux and N. Alamanos, Eur. Phys. J. A **51**, 91 (2015).
[48] I. Hamamoto, Phys. Rev. C **76**, 054319 (2007).